

## Article

# Liquid Air Energy Storage Model for Scheduling Purposes in Island Power Systems

Mohammad Rajabdorri \*, Lukas Sigrist and Enrique Lobato 

Instituto de Investigación Tecnológica (IIT), Universidad Pontificia Comillas, 28015 Madrid, Spain

\* Correspondence: mrajabdorri@comillas.edu

**Abstract:** Moving towards clean energy generation seems essential. To do so, renewable energy penetration is growing in the power systems. Although energy sources such as wind and solar are clean, they are not available consistently. Using energy storage will help to tackle variability. Liquid air energy storage is gaining attention among different energy storage technologies, as it is a promising option for grid-scale energy storage. This paper presents a detailed mixed integer linear model of liquid air energy storage to be used in scheduling and planning problems. A comprehensive cycle diagram of different processes of liquid air energy storage is presented, and a model has been developed accordingly. Simulations of the proposed model are carried out for the power system of Tenerife island and compared with the basic models. Basic models overlook specific characteristics of liquid air energy storage systems, such as charging and discharging start energy. Results confirm that the use of simple models will lead to misleading conclusions and overestimate the economic benefits of liquid air energy storage.

**Keywords:** LAES; energy storage; renewable generation; unit commitment problem



**Citation:** Rajabdorri, M.; Sigrist, L.; Lobato, E. Liquid Air Energy Storage Model for Scheduling Purposes in Island Power Systems. *Energies* **2022**, *15*, 6958. <https://doi.org/10.3390/en15196958>

Academic Editors: Thomas Kienberger and Sonja Wogrin

Received: 5 September 2022

Accepted: 20 September 2022

Published: 22 September 2022

**Publisher's Note:** MDPI stays neutral with regard to jurisdictional claims in published maps and institutional affiliations.



**Copyright:** © 2022 by the authors. Licensee MDPI, Basel, Switzerland. This article is an open access article distributed under the terms and conditions of the Creative Commons Attribution (CC BY) license (<https://creativecommons.org/licenses/by/4.0/>).

## 1. Introduction

Generating electricity has been reliant on burning fuels for decades. Although thermal generation is cheap, it emits a considerable amount of greenhouse gasses, which have negative environmental impacts. To go towards cleaner ways of generating electricity, the share of renewable energy sources (RES) is increasing in the power systems in the recent decades. Contrary to the thermal generation that can provide as much as it is demanded, renewable sources only produce energy when they are available. The abundance of available renewable energy might happen in low-demand hours, or there might be a lack of renewable production in high-demand hours. To use available RES more efficiently, it is wise to store energy when there is a surplus and inject it when required.

Different types of energy storage systems (ESS) are used in the power system, including electrochemical and battery, thermochemical, flywheel, compressed air, liquid air, magnetic, etc. [1]. There is a wide range of benefits that can be expected from energy storage systems, including load balance when the demand changes, providing additional energy to end-users during overload situations, and storing the excess energy of RES to minimize CO<sub>2</sub> emission [2]. In [3], a demand management model for industrial parks considering the integrated demand response of combined heat and power (CHP) units and thermal storage is proposed to reduce the peak demand charge.

Among different technologies, liquid air energy storage (LAES) seems promising for large-scale energy storage. Chemical energy storage systems, such as batteries, have the highest efficiency, but their short lifetime makes them expensive. In addition, they should be recycled when their life is over, which has negative environmental impacts. Large-scale mechanical storage systems such as pumped hydroelectric energy storage (PHES) and compressed air energy storage (CAES) have geographical limitations, as they need big vessels or underground caverns. These disadvantages of other technologies have led LAES

to get more attention in the research field recently, although the round-trip efficiency of LAES is lower than some of the other competing technologies [4]. Innovations are being proposed to enhance the efficiency of LAES ([5,6]). As stated in [5], disadvantages of LAES are the relatively high investment cost, large-scale requirements, and low round-trip efficiency. On the other hand, the advantages of LAES are high energy density, low storage losses, and not having geographical limitations. LAES can also help with the inertia scarcity, as the generation side is synchronous with the system. Other expected benefits are facilitating voltage control, helping with the grid restoration after outages, and introducing some reserve power.

A hybrid system of LAES combined with high-temperature thermal energy storage (HTES) is presented in [7]. HTES is used as an alternative to the conventional combustion chamber in LAES. In [8,9], liquefied natural gas (LNG) is integrated with liquid air energy storage (LAES), achieves better generation flexibility, increases operating profits from electricity arbitrage, and enhances energy efficiency. LNG is regasified depending on the amount of demand: LNG cold energy is recovered and stored during peak times, and during off-peak times, it transfers high-grade cold energy to LAES for energy storage. A combination of gas-steam combined cycle unit and LAES is proposed in [10], to better utilize the exhaust heat of the combined cycle unit and the high-grade cold energy from the liquified natural gas terminal. It is demonstrated that the integrated system is economically more efficient and also prevents temperature increases.

While innovative solutions are being proposed to make energy storage systems more feasible, it is necessary to also incorporate them into the power production scheduling and planning process. The power production problem is usually modeled as a mixed integer linear (MIL) problem; so, an MIL model of the energy storage system is very useful. In [11], the methods of incorporating ESS in the UC problem are reviewed. A general formulation of additional constraints for ESS in UC is presented, including state of charge of storage, maximum charge and discharge, binary logic, and ramping. While this general model is usually used for battery energy storage systems (BESS), more accurate models for pumped hydro storage (PSH), hydrogen storage system (HSS), and superconducting magnetic energy storage (SMES) are also presented. An interval unit commitment (IUC) model for optimal energy and reserve scheduling in a system with CAES is introduced in [12], which also considers frequency dynamics. A robust optimization approach is employed in [13], to achieve the offering and bidding curves of CAES. In both of these studies with CAES, a general MIL model is used that overlooks the charging and discharging start energy of CAES and transitions. The reviewed literature is categorized and summarized in Figure 1.

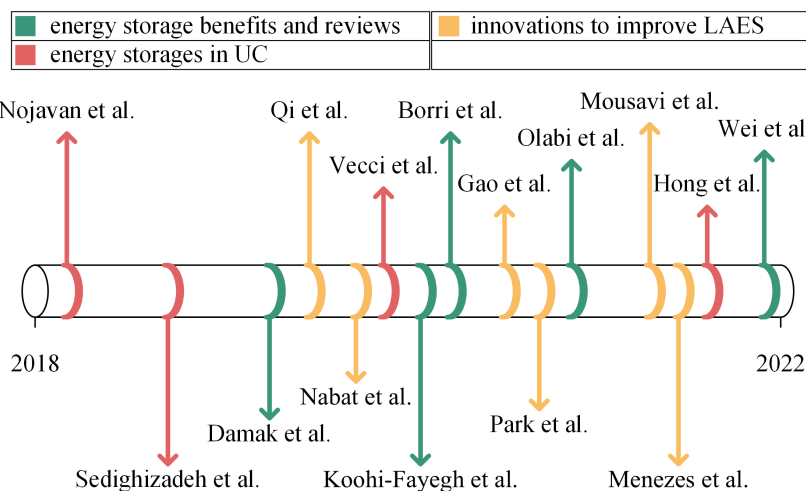


Figure 1. Summary of references [1–15].

This paper introduces a detailed MIL model for LAES to incorporate into the UC problem, which includes charging and discharging start energies of LAES. To the best

of the authors' knowledge, an explicit LAES model has never been investigated in the literature. The contribution of this paper is presenting an MIL formulation of LAES that includes charging start energy (CSE) and discharging start energy (DSE). Realistic future scenarios of Tenerife island for the years 2026 and 2030 are used to validate the proposed model, by solving weekly UC. As wind and solar availability vary from season to season, weekly sample scenarios of winter, spring, summer, and autumn are used to provide a better insight over each year. The model is compared with the general formulation, and the differences are pointed out.

The methodology, including basic and proposed LAES formulation, is presented in Section 2. Scenarios and obtained results are presented in Section 3. Then, conclusions are drawn in Section 4.

## 2. Methodology

### 2.1. UC Formulation

The short-term scheduling is often solved by the mixed integer linear formulation of the UC problem. A general formulation is presented here.

$$\begin{aligned} \min_x \text{suc}(x_{t,i}) + gc(p_{t,i}) & \quad (1) \\ x_{t,i} - x_{t-1,i} = y_{t,i} - z_{t,i} & \quad t \in \mathcal{T}, i \in \mathcal{I} \quad (1a) \\ y_{t,i} + z_{t,i} \leq 1 & \quad t \in \mathcal{T}, i \in \mathcal{I} \quad (1b) \\ \sum_{tt=t-UT_i+1}^t y_{tt,i} \leq x_{t,i} & \quad t \in \{UT_i, \dots, \mathcal{T}\} \quad (1c) \\ \sum_{tt=t-DT_i+1}^t z_{tt,i} \leq 1 - x_{t,i} & \quad t \in \{UT_i, \dots, \mathcal{T}\} \quad (1d) \\ p_{t,i} \geq \underline{P}_i \cdot x_{t,i} & \quad t \in \mathcal{T}, i \in \mathcal{I} \quad (1e) \\ p_{t,i} \leq \overline{P}_i \cdot x_{t,i} & \quad t \in \mathcal{T}, i \in \mathcal{I} \quad (1f) \\ p_{t-1,i} - p_{t,i} \leq \underline{R}_i & \quad t \in \mathcal{T}, i \in \mathcal{I} \quad (1g) \\ p_{t,i} - p_{t-1,i} \leq \overline{R}_i & \quad t \in \mathcal{T}, i \in \mathcal{I} \quad (1h) \\ r_t = \sum_{i \in \mathcal{I}} (r_{i,t}^{Ther}) + r_t^{LAES} + r_t^{BESS} & \quad t \in \mathcal{T} \quad (1i) \\ \sum_{i \in \mathcal{I}} (p_{t,i}) + wg_t + sg_t + p_t^{dischar} = \mathcal{D}_t + CSE_t + DSE_t + p_t^{char} & \quad t \in \mathcal{T} \quad (1j) \\ wg_t \leq \mathcal{W}_t & \quad t \in \mathcal{T} \quad (1k) \\ sg_t \leq \mathcal{S}_t & \quad t \in \mathcal{T} \quad (1l) \\ r_{i,t}^{Ther} = \max[\overline{P}_i \cdot x_{t,i} - p_{t,i}, \overline{R}_i \cdot x_{t,i}] & \quad (1m) \\ r_t - r_{i,t}^{Ther} \geq p_{t,i} & \quad t \in \mathcal{T}, i \in \mathcal{I} \quad (1n) \\ r_t \geq (wg_t + sg_t) \times RRM & \quad t \in \mathcal{T} \quad (1o) \end{aligned}$$

The aim is to solve Equation (1) subject to Equations (1a)–(1o).  $gc(\cdot)$  is usually a quadratic cost function, which will be piecewise linearized to be utilized in the MIL problem. The objective function of Equation (1) tends to minimize the start-up costs, plus the cost of thermal generation. Equations (1a) and (1b) represent the binary logic of the thermal units. Equations (1c) and (1d) are the minimum up-time and minimum downtime constraints of the thermal units. Equation (1e) is the minimum power generation constraint. Equation (1f) is the maximum power generation constraint. Equations (1g) and (1h) are ramp-down and ramp-up constraints. Equation (1i) is the total up reserve equation. Total reserve is the summation of generation headroom of thermal units, plus the amount of reserve that is provided by LAES and BESS. Equation (1j) is the power balance equation, considering LAES charge and discharge. It is later explained how to calculate  $CSE_t$  and  $DSE_t$ . Equations (1k) and (1l) make sure that the scheduled wind power and solar power

are always equal to or less than the forecasted amount. Equation (1m) calculates the amount of reserve that each unit can provide. Constraint Equations (1n) and (1o) are stating that the available reserve should be always bigger than any outage of thermal units and estimated intra-hour variations of renewable infeed.

## 2.2. Liquid Air Energy Storage (LAES)

### 2.2.1. LAES Model

Energy stored in the cryogen (liquefied gas) is different from other types of heat storage; it is obtained from decreasing internal energy and increasing its exergy. The principle of using liquid air to store energy is based on three steps: (a) liquefying air when energy is available, (b) storing it as a liquid in insulated vessels, and (c) expanding the air and pumping it to turbines to generate power [14]. The process is shown in Figure 2 schematically.

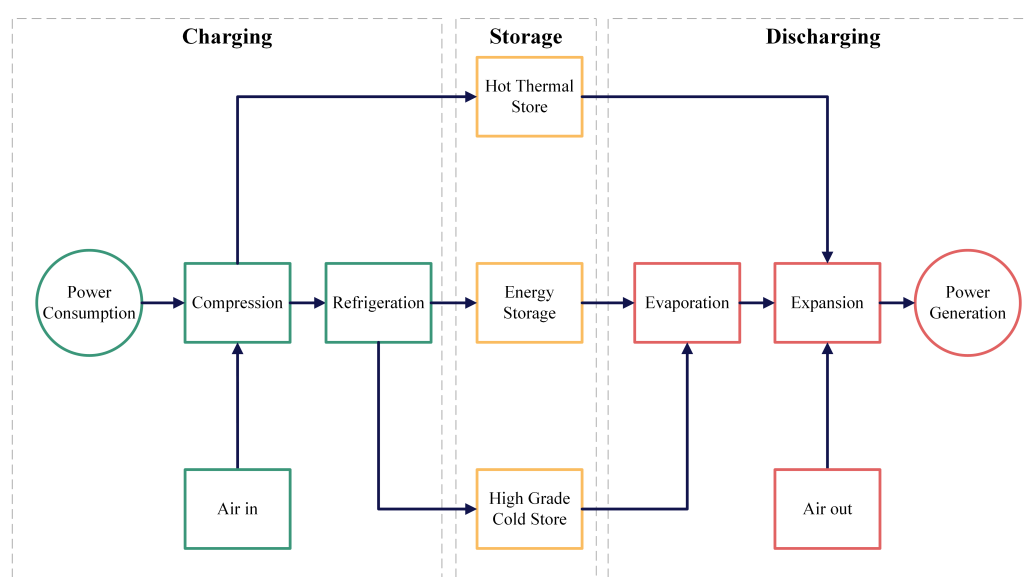


**Figure 2.** LAES process.

A detailed cycle diagram that includes transitions and start-up energies necessary to develop an MIL model of LAES. The cycle diagram of LAES is presented in Figure 3. The same duty cycle can be found in [15] for different operation modes.

In this diagram, charge start time, charge duration, charge down duration, charge-discharge turnaround time, discharge start time, discharge duration, and discharge down-time are specified. In current technologies of LAES, charge start time and energy cannot be ignored. Charge down and discharge down duration are negligible, hence ignored in this paper.

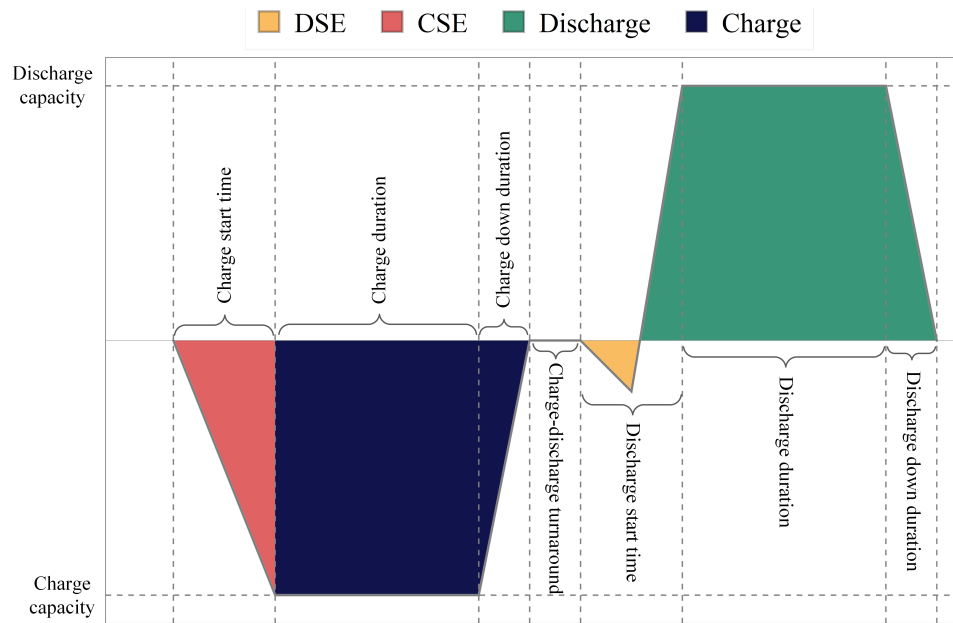


Figure 3. LAES cycle diagram.

### 2.2.2. LAES Basic Formulation

Storage devices are usually modeled with a set of constraints, presented here.

$$x_t^{char} + x_t^{dischar} \leq 1 \tag{2}$$

$$p_t^{char} \leq \overline{P}_{char}(x_t^{char}) \tag{3}$$

$$p_t^{dischar} \leq \overline{P}_{dischar}(x_t^{dischar}) \tag{4}$$

$$e_t^{LAES} = e_{t-1}^{LAES} + p_t^{char} \zeta^{LAES} - p_t^{dischar} \tag{5}$$

Equation (2) makes sure that only one of the charging or discharging modes is active. Equations (3) and (4) are the maximum charging and discharging capacity of LAES, respectively. In addition, in (5), the energy state of LAES is defined.

Using this approach for LAES ignores the charging start-up energy, discharging start-up energy, transient ramp up and ramp down, the turnaround times, minimum charging, and minimum discharging. These differences can add up and lead to unrealistic conclusions regarding the planning and scheduling LAES.

### 2.2.3. LAES Proposed Formulation

Due to essential differences between liquid air systems and batteries, ignoring the characteristics of LAES may lead to unrealistic results. Here, an accurate model of LAES is presented that takes into account the unique characteristics of LAES. To define the binary logic, it should be noted that: (a) simultaneous charging and discharging are not allowed; (b) charge start energy and discharge start energy are imperative; so, binary variables of charging start-up, charging shut-down, discharging start-up, and discharging shut-down should also be defined.

$$x_t^{char} + x_t^{dischar} \leq 1 \tag{6}$$

$$x_t^{char} - x_{t-1}^{char} = y_t^{char} - z_t^{char} \tag{7}$$

$$y_t^{char} + z_t^{char} \leq 1 \tag{8}$$

$$x_t^{dischar} - x_{t-1}^{dischar} = y_t^{dischar} - z_t^{dischar} \tag{9}$$

$$y_t^{dischar} + z_t^{dischar} \leq 1 \tag{10}$$

Simultaneous charging and discharging are avoided by Equation (6). In Equations (7) and (8), the binary logic for start-up and shut-down of charging mode is defined. The same logic is defined for the discharging mode in Equations (9) and (10).

Other than maximum capacity for charging and discharging, LAES is limited with minimum charging and discharging boundaries, too. Especially in the charging mode, LAES should always be charged close to maximum capacity. The capacity constraints are presented here.

$$p_t^{char} \leq \overline{\mathcal{P}}_{char} (x_t^{char} - y_t^{char} \times CST) \quad (11)$$

$$p_t^{char} \geq \underline{\mathcal{P}}_{char} (x_t^{char} - y_t^{char} \times CST) \quad (12)$$

$$p_t^{dischar} \leq \overline{\mathcal{P}}_{dischar} (x_t^{dischar} - y_t^{dischar} \times DST) \quad (13)$$

$$p_t^{dischar} \geq \underline{\mathcal{P}}_{dischar} (x_t^{dischar} - y_t^{dischar} \times DST) \quad (14)$$

Charging is limited by the maximum charge capacity of LAES in Equation (11). However, it always takes a while to start up the charging process. Depending on the LAES technology, charging start time might vary from minutes to more than half an hour. CST stands for charging start time and indicates what fraction of an hour it takes for the charging process to start up. Minimum charge capacity is imposed in Equation (12). Maximum and minimum discharge capacities are defined in the same manner in Equations (13) and (14).

$$e_t^{LAES} = e_{t-1}^{LAES} + p_t^{char} \zeta^{LAES} - p_t^{dischar} \quad (15)$$

$$e_0^{LAES} = e_T^{LAES} \quad (16)$$

The energy state of LAES is calculated with Equation (15). Equation (16) makes sure that the energy state at the beginning and end of the time horizon is equal. As mentioned before, the amount of charging start energy and discharging start energy are not negligible in LAES, and should be taken into account.

$$CSE_t = CSP \times CST \times \overline{\mathcal{P}}_{char} \times y_t^{char} \quad (17)$$

$$DSE_t = DSP \times DST \times \overline{\mathcal{P}}_{dischar} \times y_t^{dischar} \quad (18)$$

Charging start energy (CSE) is calculated in Equation (17) for each hour, considering charging start power (CSP) and charging start time (CST). Discharging start energy (DSE) is calculated in Equation (18) for each hour, considering discharging start power (DSP) and discharging start time (CST). Compared to other fast storage devices, LAES does not contribute a lot to the primary reserve provision. Depending on the acceptable duration of the primary response, the reserve provided by LAES can be calculated as follows:

$$r_t^{LAES} = CSE_t + p_t^{char} + \max[\overline{\mathcal{R}}_{dischar} \cdot x_t^{dischar}, \overline{\mathcal{P}}_{dischar} \cdot x_t^{dischar} - p_t^{dischar}] \times PRD \quad (19)$$

The amount of reserve that LAES provides is the sum of charging power (because it can instantaneously stop charging) and the maximum between up ramp and capacity headroom, multiplied by primary response duration (PRD). The slower ramp-up speed of LAES in comparison with BESS is the main reason why it is usually implemented alongside a BESS with a low energy capacity. So, LAES can store the curtailed RES in high penetration hours, and BESS can provide the fast response that is needed in case of any contingency.

The MIL formulation of LAES that is presented in Equations (6) to (19) is added to the UC optimization problem in Equation (1), to schedule the LAES optimally.

### 3. Results

To point out the differences that the proposed LAES model can make, simulations are carried out for the Tenerife Island power system, with the forecasted data of 2026 and 2030.

As the RES input is widely different throughout the year, sample weeks of each season are considered. The scaled amount of demand for 2026 is shown in Figure 4, numbers are scaled up for 2030 according to annual energy consumption forecasts. Wind and solar profiles are shown in Figures 5 and 6, respectively, in per unit of installed capacity. Wind and solar capacities for 2026 and 2030 are in accordance with the most recent estimations of Red Eléctrica de España [16].

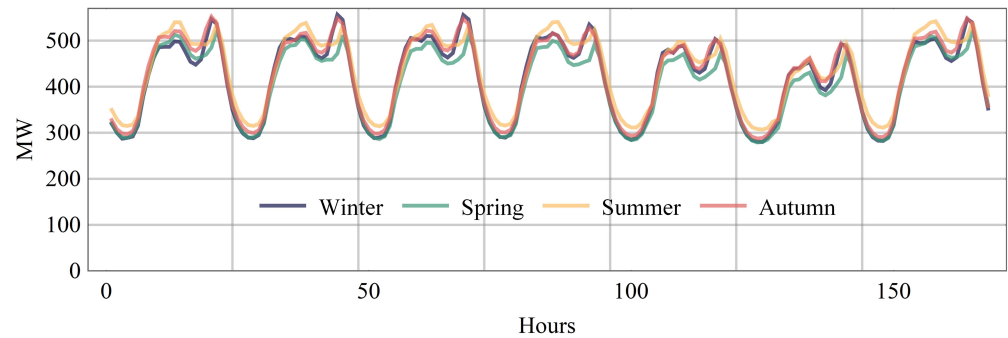


**Figure 4.** Estimated demand of 2026 for a sample week of winter, spring, summer, and autumn.

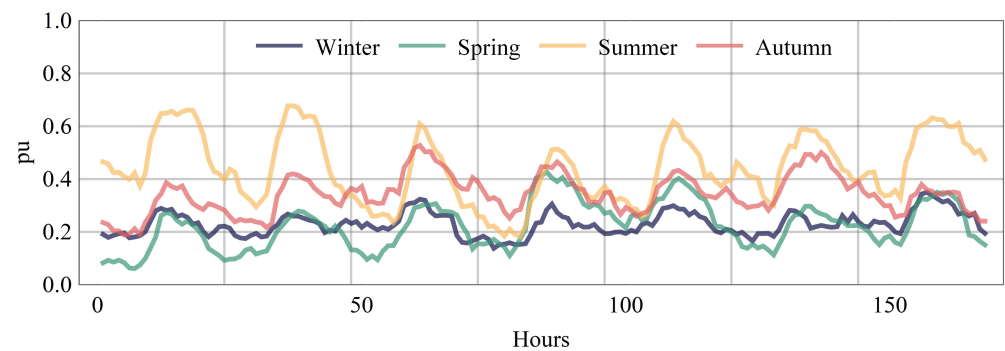


**Figure 5.** Estimated wind generation for sample weeks of winter, spring, summer, and autumn, in per unit.

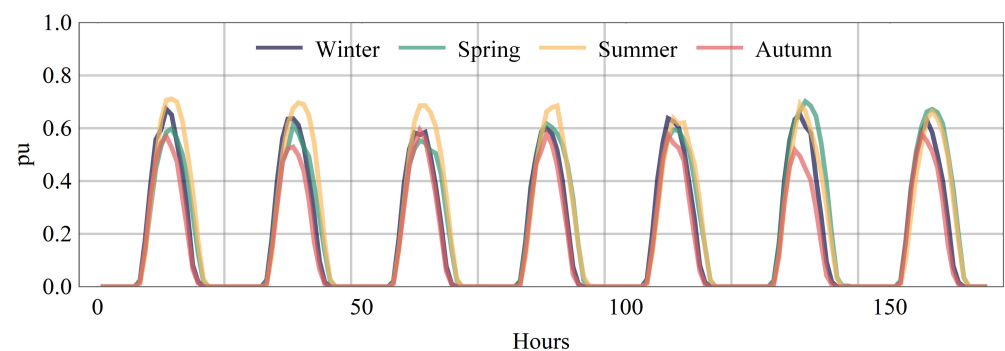


**Figure 6.** Estimated solar generation for sample weeks of winter, spring, summer, and autumn, in per unit.

Considering that the LAES is too slow to provide a significant amount of primary reserve, in practice, it is usually supported by a low-capacity, fast BESS. The idea is to perform load shifting and RES storage on high penetration hours with the LAES (because it has a big capacity) and put the low capacity BESS on hold for contingencies and moments with up reserve shortage. So, in this study, we assume that every LAES is accompanied by a BESS as big as the LAES maximum charging capacity. To be able to fully capture the differences that a more accurate LAES formulation can make, for each time horizon (different seasons of 2026 and 2030), five scenarios are considered:

**No LAES (base case):** There is no LAES and no BESS in this scenario. It serves as the base case.

**A 50 MW LAES, basic model (50 MW BM):** In this scenario, LAES with 50 MW/h maximum charging capacity and 300 MWh energy capacity is installed in the system, which is supported by a 50 MWh energy capacity BESS. The BESS only provides reserve. The basic LAES model is used in the formulation.

**A 50 MW LAES, the proposed model (50 MW PM):** In this scenario, LAES with 50 MW/h maximum charging capacity and 300 MWh energy capacity is installed in the system, which is supported by a 50 MWh energy capacity BESS. The BESS only provides reserve. The proposed LAES model is used in the formulation.

**A 100 MW LAES, basic model (100 MW BM):** In this scenario, LAES with 100 MW/h maximum charging capacity and 600 MWh energy capacity is installed in the system, which is supported by a 100 MWh energy capacity BESS. The BESS only provides reserve. The basic LAES model is used in the formulation.

**A 100 MW LAES, the proposed model (100 MW PM):** In this scenario, LAES with 100 MW/h maximum charging capacity and 600 MWh energy capacity is installed in the system, which is supported by a 100 MWh energy capacity BESS. The BESS only provides reserve. The proposed LAES model is used in the formulation.

A summary of the input properties used for LAES is presented in Table 1.

**Table 1.** LAES properties.

$\zeta^{LAES}$	55%
CST	30 min
DST	$\overline{P}_{dischar}/5 \text{ MW min}$
CSE PM	$60\% \times \overline{P}_{char} \times CST$
DSE	$0.5\% \times \overline{P}_{dischar} \times DST$
Charge and discharge rundown time	0

How LAES participates in the power balance in different scenarios is shown in Figure 7, for a sample week of summer 2030.

As expected, there is much more curtailed RES when there is no LAES and BESS installed. Mainly because more thermal generation is forced to be online to provide the required up reserve. In the middle of the day when there is more solar power injection or windy hours, thermal generation goes down as much as possible, while there is enough headroom to comply with the reserve criteria. The rest of the available RES is curtailed. When LAES is added to save extra RES when necessary, and BESS is added to provide a reserve, thermal generation can go even lower, to better utilize available RES. A 50 MW LAES is able to store some of the extra RES, but still at some hours, with so much RES injection, there would be curtailment. The main difference between the proposed model and the basic model is the amount of CSE. DSE is also calculated, but the amount is much less than the CSE. Comparing the cases with the proposed model, and cases with the basic model in Figure 7, the amount of curtailment in the proposed model seems larger. This is mainly because CSE and DSE consume extra energy. In addition, the number of start-ups in the LAES is reduced with the proposed model, to avoid CSE as much as possible.

To see the differences that the proposed model makes, specifically in the charging and discharging pattern of LAES, the results for a sample summer week of 2030, with 100 MW LAES installed, are depicted in Figures 8 and 9.

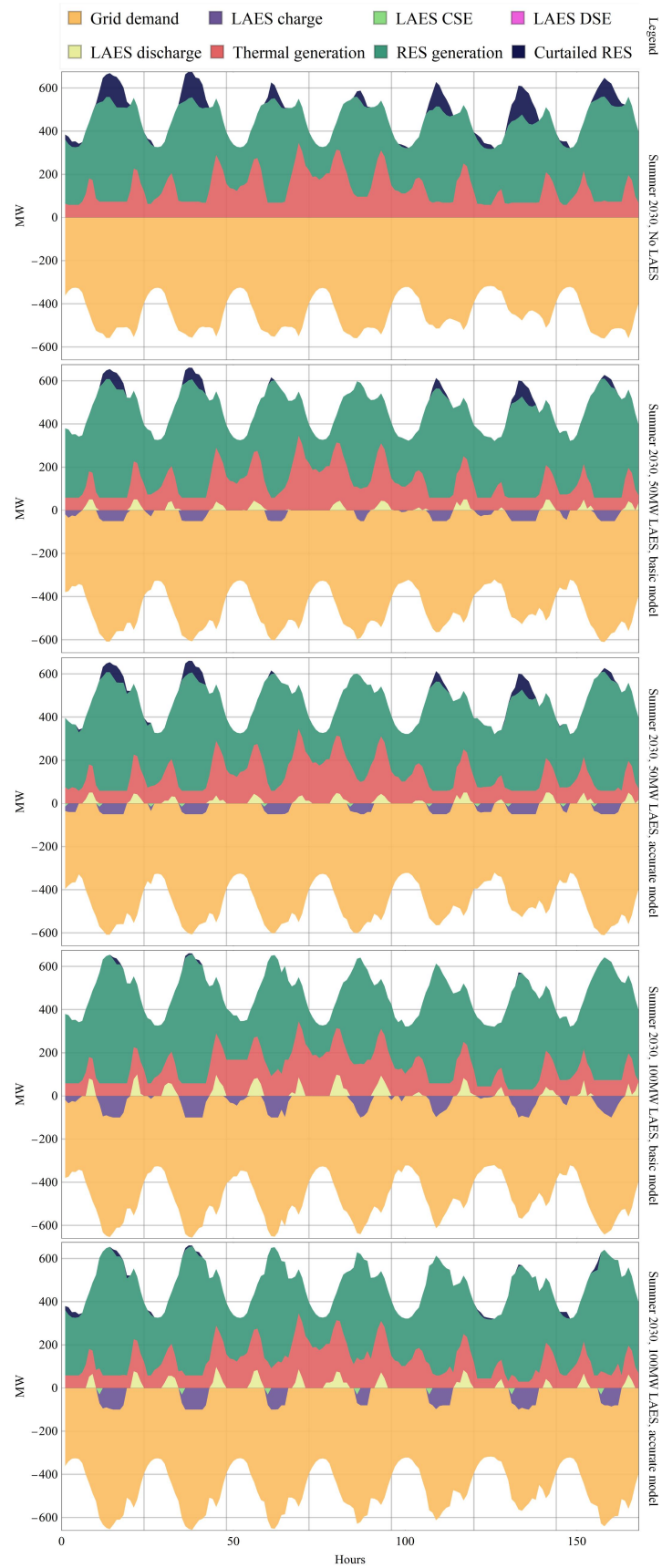
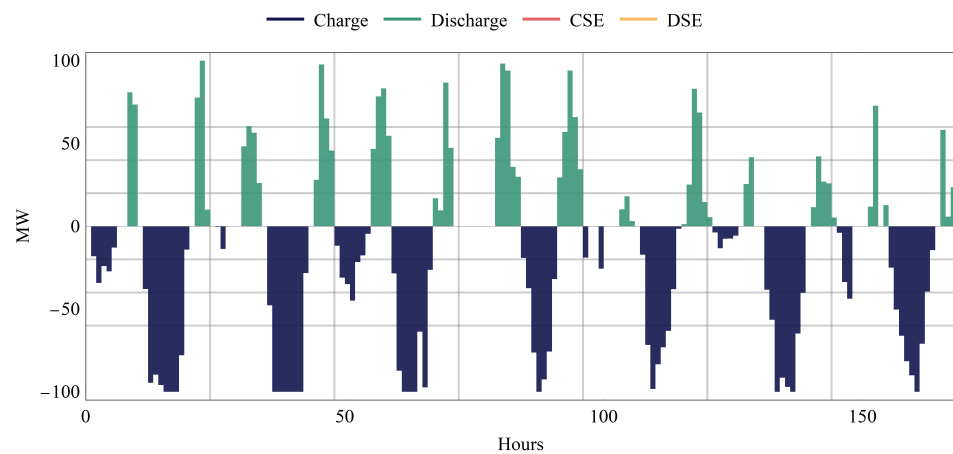
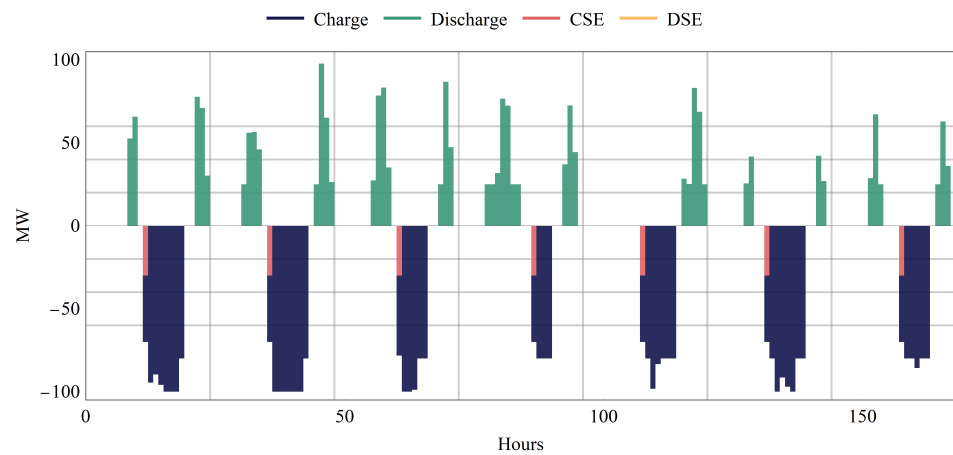


Figure 7. Power balance, sample week of summer 2030.



**Figure 8.** LAES charging-discharging, sample week of summer 2030, basic model.



**Figure 9.** LAES charging-discharging, sample week of summer 2030, proposed model.

The DSE is so small that it cannot be seen in the figures. However, CSE can effectively reduce the number of charging incidents to avoid unnecessary CSE as much as possible. In addition, there are many hours in the basic model, and LAES is scheduled with a low amount of charging. In practice, the current technology of LAES is usually only able to charge close to maximum capacity (80% of maximum charging capacity or more).

From the weekly UC solutions of winter, spring, summer, and autumn sample weeks, an estimated yearly summary of results for years 2026 and 2030 is presented in Tables 2 and 3.

**Table 2.** Yearly Results of 2026.

	Operation Cost (k€)	Scheduled RES (GW)	Number of Charging	Number of Discharging
base case	205,600	1877.3	-	-
50 MW BM	181,215	1898.8	912	847
50 MW PM	188,434 (+3.4%)	1898.7 (0.0%)	508 (−44.3%)	834 (−1.5%)
100 MW BM	177,514	1900.4	847	769
100MW PM	183,413 (+3.3%)	1900.3 (0.0%)	365 (−56.9%)	730 (−5.1%)

**Table 3.** Yearly Results of 2030.

	Operation Cost (k€)	Scheduled RES (GW)	Number of Charging	Number of Discharging
base case	192,618	2127.7	-	-
50 MW BM	168,753	2175.2	939	873
50 MW PM	169,130 (+0.2%)	2174.4 (−0.0%)	560 (−40.4%)	795 (−15.3%)
100 MW BM	162,647	2191.6	847	872
100 MW PM	165,001 (+1.4%)	2188.0 (−0.2%)	469 (−44.6%)	730 (−16.3%)

Although the operation cost is reduced for cases with storage systems compared to the base case with no storage system, the basic model always underestimates the operation costs. With the detailed model, the operator will have a more accurate power balance schedule, and a better awareness of expected losses. An incremental or decreasing percentage is also provided in both tables, which compare the basic model and the proposed model. According to the tables, the basic model can be misleading in reflecting the realistic operation cost. In addition, as the CSE and DSE are taken into account in the proposed model, the number of scheduled charging periods is diminished considerably in the proposed model. It also reduces the wear and tear of LAES in practice. It would also be interesting to see how much CSE consumption is overlooked by the basic model yearly. The corresponding numbers are presented in Table 4. These yearly amounts might seem small. So, for the long-term planning procedures in which these orders are negligible, the simple model can be a good choice, as it is less complicated and this might affect the speed of big long-term problems. On the other hand, for short-term scheduling problems, the proposed model can help to avoid unnecessary real-time modifications. All of the UC problems in this paper are solved by the cplex solver in GAMS.

**Table 4.** Overlooked yearly CSE consumption in the basic model.

	50 MW BM (2026)	100 MW BM (2026)	50 MW BM (2030)	100 MW BM (2030)
Yearly CSE	13,680 MW	25,410 MW	14,085 MW	25,410 MW

#### 4. Conclusions

The benefits and ancillary services that LAES provides are manifold and are not limited to cost reduction. However, to prevent the overestimation of the operation cost reduction with LAES in the system, a detailed representation of LAES in the UC problem is needed. A detailed model can take other characteristics of LAES, such as CSE and DSE into account. This will give more accurate insight to the operator or the planners. In addition, with a basic model, LAES will be scheduled to start up too many times, which in reality imposes a lot of charging and discharging start energy. The proposed model gives a realistic awareness of the cost and benefits of LAES, and by considering CSE, automatically prevents unnecessary start-ups to minimize unnecessary energy losses.

**Author Contributions:** Methodology, M.R.; software, M.R., E.L., L.S.; validation, L.S., E.L.; investigation, M.R.; data curation, M.R.; writing—original draft preparation, M.R.; writing—review and editing, L.S. and E.L.; visualization, M.R.; supervision, L.S. and E.L. All authors have read and agreed to the published version of the manuscript.

**Funding:** This study has been partially funded by the European Regional Development Fund (ERDF), Ministerio de Ciencia e Innovación—Agencia Estatal de Investigación, Project RTI2018-100965-A-I00 and by MCIN/AEI/ 10.13039/501100011033.

**Informed Consent Statement:** Not applicable.

**Data Availability Statement:** Not applicable.

**Conflicts of Interest:** The funders had no role in the design of the study; in the collection, analyses, or interpretation of data; in the writing of the manuscript; or in the decision to publish the results.

## Nomenclature

### Acronyms

BESS	battery energy storage systems
CAES	compressed air energy storage
CHP	combined heat and power
CSE	charging start energy
CSP	charging start power
CST	charging start time
DSE	discharging start energy
DSP	discharging start power
DST	discharging start time
EES	energy storage system
HSS	hydrogen storage system
HTES	high-temperature thermal energy storage
IUC	interval unit commitment
LAES	liquid air energy storage
LNG	liquefied natural gas
MIL	mixed integer linear
PHES	pumped hydroelectric energy storage
PRD	primary response duration
RES	renewable energy source
RRM	renewable reserve multiplier
SMES	superconducting magnetic energy storage
UC	unit commitment

### Indices

$i$	index of generators
$ii$	alias index for generators
$t$	index of time intervals
$tt$	alias index for time intervals

### Parameters

$\mathcal{D}$	power demand [MW]
$\mathcal{I}$	number of generators
$\mathcal{S}$	available solar [MW]
$\mathcal{T}$	time period
$\mathcal{W}$	available wind [MW]
$\overline{P}_i$	maximum power output of generator $i$ [MW]
$\overline{P}_{char}$	LAES maximum charging [MW]
$\overline{P}_{dischar}$	LAES maximum discharging [MW]
$\overline{R}_i$	maximum ramp-up of generator $i$ [MW]
$\underline{p}^{char}$	LAES minimum charging [MW]
$\underline{p}^{dischar}$	LAES minimum discharging [MW]
$\underline{P}_i$	minimum power output of generator $i$ [MW]
$\underline{R}_i$	maximum ramp-down of generator $i$ [MW]
$\xi^{LAES}$	LAES round-trip efficiency
$DT$	minimum down-time of generators [hours]
$UT$	minimum up-time of generators [hours]

### Variables

$e^{LAES}$	LAES energy state [MW]
$gc$	generation costs [€]
$p$	thermal power generation [MW]
$p^{char}$	LAES charge power [MW]
$p^{dischar}$	LAES discharge power [MW]
$r$	online reserve power [MW]

$r^{BESS}$	BESS power reserve [MW]
$r^{LAES}$	LAES power reserve [MW]
$r^{Ther}$	thermal power reserve [MW]
$sg$	solar generation [MW]
$suc(.)$	start-up costs [€]
$wg$	wind generation [MW]
$x$	thermal unit status [ $\in\{0,1\}$ ]
$x^{char}$	LAES charging status [ $\in\{0,1\}$ ]
$x^{dischar}$	LAES discharging status [ $\in\{0,1\}$ ]
$y$	thermal unit start-up [ $\in\{0,1\}$ ]
$y^{char}$	LAES charging start-up [ $\in\{0,1\}$ ]
$y^{dischar}$	LAES discharging start-up [ $\in\{0,1\}$ ]
$z$	thermal unit shut-down [ $\in\{0,1\}$ ]
$z^{char}$	LAES charging shut-down [ $\in\{0,1\}$ ]
$z^{dischar}$	LAES discharging shut-down [ $\in\{0,1\}$ ]

## References

- Koohi-Fayegh, S.; Rosen, M.A. A review of energy storage types, applications and recent developments. *J. Energy Storage* **2020**, *27*, 101047. [[CrossRef](#)]
- Olabi, A.; Onumaegbu, C.; Wilberforce, T.; Ramadan, M.; Abdelkareem, M.A.; Al-Alami, A.H. Critical review of energy storage systems. *Energy* **2021**, *214*, 118987. [[CrossRef](#)]
- Wei, J.; Zhang, Y.; Wang, J.; Wu, L.; Zhao, P.; Jiang, Z. Decentralized Demand Management Based on Alternating Direction Method of Multipliers Algorithm for Industrial Park with CHP Units and Thermal Storage. *J. Mod. Power Syst. Clean Energy* **2022**, *10*, 120–130. [[CrossRef](#)]
- Borri, E.; Tafone, A.; Romagnoli, A.; Comodi, G. A review on liquid air energy storage: History, state of the art and recent developments. *Renew. Sustain. Energy Rev.* **2021**, *137*, 110572. [[CrossRef](#)]
- Menezes, M.V.P.; Vilasboas, I.F.; da Silva, J.A.M. Liquid Air Energy Storage System (LAES) Assisted by Cryogenic Air Rankine Cycle (ARC). *Energies* **2022**, *15*, 2730. [[CrossRef](#)]
- Mousavi, S.B.; Nabat, M.H.; Razmi, A.R.; Ahmadi, P. A comprehensive study and multi-criteria optimization of a novel sub-critical liquid air energy storage (SC-LAES). *Energy Convers. Manag.* **2022**, *258*, 115549. [[CrossRef](#)]
- Nabat, M.H.; Zeynalian, M.; Razmi, A.R.; Arabkoohsar, A.; Soltani, M. Energy, exergy, and economic analyses of an innovative energy storage system; liquid air energy storage (LAES) combined with high-temperature thermal energy storage (HTES). *Energy Convers. Manag.* **2020**, *226*, 113486. [[CrossRef](#)]
- Qi, M.; Park, J.; Kim, J.; Lee, I.; Moon, I. Advanced integration of LNG regasification power plant with liquid air energy storage: Enhancements in flexibility, safety, and power generation. *Appl. Energy* **2020**, *269*, 115049. [[CrossRef](#)]
- Park, J.; Cho, S.; Qi, M.; Noh, W.; Lee, I.; Moon, I. Liquid air energy storage coupled with liquefied natural gas cold energy: Focus on efficiency, energy capacity, and flexibility. *Energy* **2021**, *216*, 119308. [[CrossRef](#)]
- Gao, Z.; Ji, W.; Guo, L.; Fan, X.; Wang, J. Thermo-economic analysis of the integrated bidirectional peak shaving system consisted by liquid air energy storage and combined cycle power plant. *Energy Convers. Manag.* **2021**, *234*, 113945. [[CrossRef](#)]
- Hong, Y.Y.; Apolinario, G.F.D.; Lu, T.K.; Chu, C.C. Chance-constrained unit commitment with energy storage systems in electric power systems. *Energy Rep.* **2022**, *8*, 1067–1090. [[CrossRef](#)]
- Sedighzadeh, M.; Esmaili, M.; Mousavi-Taghiabadi, S.M. Optimal joint energy and reserve scheduling considering frequency dynamics, compressed air energy storage, and wind turbines in an electrical power system. *J. Energy Storage* **2019**, *23*, 220–233. [[CrossRef](#)]
- Nojavan, S.; Najafi-Ghalelou, A.; Majidi, M.; Zare, K. Optimal bidding and offering strategies of merchant compressed air energy storage in deregulated electricity market using robust optimization approach. *Energy* **2018**, *142*, 250–257. [[CrossRef](#)]
- Damak, C.; Leducq, D.; Hoang, H.M.; Negro, D.; Delahaye, A. Liquid Air Energy Storage (LAES) as a large-scale storage technology for renewable energy integration—A review of investigation studies and near perspectives of LAES. *Int. J. Refrig.* **2020**, *110*, 208–218. [[CrossRef](#)]
- Vecchi, A.; Li, Y.; Mancarella, P.; Sciacovelli, A. Integrated techno-economic assessment of Liquid Air Energy Storage (LAES) under off-design conditions: Links between provision of market services and thermodynamic performance. *Appl. Energy* **2020**, *262*, 114589. [[CrossRef](#)]
- REE. *Estudios de Prospectiva del Sistema y Necesidades Para su Operabilidad*; REE: Herzliya, Israel, 2020.